

Suppression of crystalline fluctuations by competing structures in a supercooled liquid

Pierre Ronceray

Princeton Center for Theoretical Science, Princeton University, Princeton, New Jersey 08544, USA

Peter Harrowell

School of Chemistry, University of Sydney, Sydney, New South Wales 2006, Australia

(Received 19 June 2017; published 6 October 2017)

We propose a geometrical characterization of amorphous liquid structures that suppress crystallization by competing locally with crystalline order. We introduce for this purpose the *crystal affinity* of a liquid, a simple measure of its propensity to accumulate local crystalline structures on cooling. This quantity is explicitly related to the high-temperature structural covariance between local fluctuations in crystal order and that of competing liquid structures: favoring a structure that, due to poor overlap properties, anticorrelates with crystalline order reduces the affinity of the liquid. Using a lattice model of a liquid, we show that this quantity successfully predicts the tendency of a liquid to either accumulate or suppress local crystalline fluctuations with increasing supercooling. We demonstrate that the crystal affinity correlates strongly with the crystal nucleation rate and the crystal-liquid interfacial free energy of the low-temperature liquid, making our theory a predictive tool to determine which amorphous structures enhance glass-forming ability.

DOI: [10.1103/PhysRevE.96.042602](https://doi.org/10.1103/PhysRevE.96.042602)

I. INTRODUCTION

The ultimate fate of a liquid upon slow cooling—whether it crystallizes or arrests into an amorphous glass—depends on how easily the crystal can nucleate in the supercooled liquid. It has long been speculated that this kinetic stability with respect to crystallization can be related to the geometrical properties of the local structures which, at the molecular scale, are particularly stable. More specifically, such favored local structures that are geometrically adverse to crystallinity—for instance, due to noncrystalline symmetries—would enhance the stability of the liquid. This idea can be traced back to Frank’s 1952 proposal [1] that the stability of icosahedral coordination shells in pure metallic liquids might impede crystallization of close packed cubic crystals. From this starting point, a substantial literature has developed [2,3], exploring a variety of approaches to the nature and influence of liquid structure. This includes the study of geometrical frustration in liquids [4], the descriptive study of the distribution of local coordination structures in liquids via computer simulations [5], and, recently, nanofocused electron scattering [6], and the search for correlation between specific local structures and the local relaxation rates [7].

In spite of this considerable activity, explicit evidence of the essential thesis, that there is a correlation between liquid structure and crystallization kinetics, remains sparse. Taffs and Royall [8] have reported on the crystallization of a hard sphere liquid subjected to a bias that favors fivefold common neighbor coordination. They established a clear dependence of the reduced crystallization time on the magnitude of the bias field, confirming that the liquid structure does indeed influence the rate of crystallization. The clear result of Ref. [8] is something of an exception: generally, any adjustment of the Hamiltonian to vary the liquid structure also changes the stability of the crystal structure, along with that of any polymorph favored by the perturbation. For example, Molinero *et al.* [9] found that adjusting the strength λ of the three-body contribution in a

model of silicon potential resulted in a maximal glass-forming ability that coincided with the value of λ corresponding to the crossover in stable crystal phases. As this point coincides with the maximal depression of the freezing point, it is difficult to disentangle the role of liquid structure from that of crystal stability. A similar issue has arisen in experimental efforts to confirm the influence of liquid structure. Lee *et al.* [10] studied the kinetics of crystal nucleation in a Ti-Zr-Ni alloy in which the degree of local icosahedral order could be varied with composition. Here the increase in liquid icosahedral order coincided with stabilization of a quasicrystal whose nucleation rate was significantly greater than that of the cubic crystal, effectively concealing whatever influence the liquid structure had on the crystallization of the latter crystal.

II. THE FAVORED LOCAL STRUCTURES MODEL

To summarize the discussion above, to establish the influence of liquid structure on crystallization kinetics we would like to be able to vary the liquid structure as freely as possible while still ensuring that the equilibrium crystal state remains unchanged. The aim of this article is to present both a model that satisfies these conditions and a theoretical framework relating the local geometrical properties of stable liquid structures to the crystal nucleation rate. To this end, we utilize a simple lattice model, the favored local structures (FLS) model [11–13]. We consider binary spins, representing some local conformational degree of freedom of the liquid (e.g., composition), on a face-centered cubic lattice. We define the *local structure* of the liquid at a given site as the geometrical arrangement of the 12 spins surrounding it. There are 218 rotationally distinct structures at this nearest-neighbor level, and we associate an energy ϵ_i to each site with local structure i . Our model therefore has 218 variable energy levels corresponding to the possible local structures. The set of energies $\{\epsilon_i\}_{i=1,\dots,218}$ constitutes the *local energy landscape* and entirely characterizes the system’s Hamiltonian. The

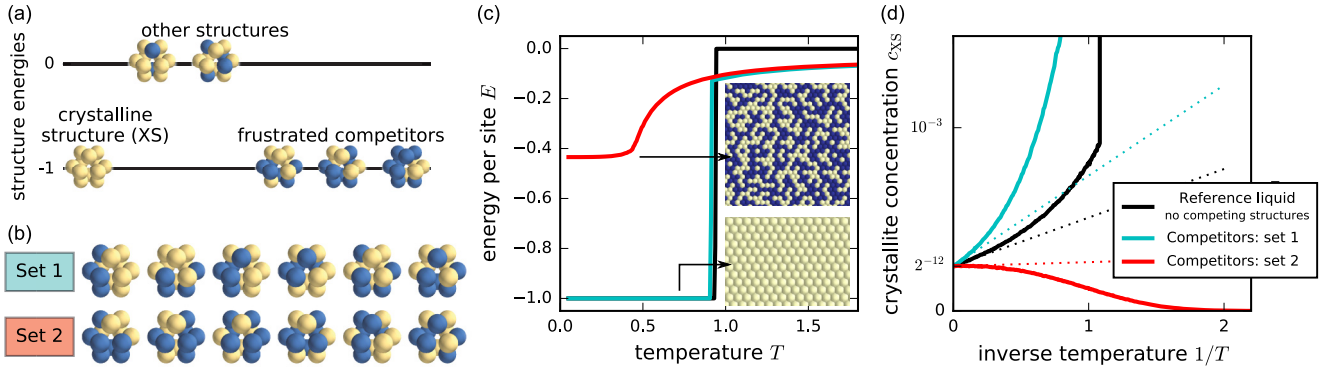


FIG. 1. (a) An illustration of the local energy landscape where the crystalline structure (XS) and a number n of competitors have an energy of -1 , while other structures have zero energy. (b) Two sets of $n = 6$ competitors. (c) Average energy per site as a function of temperature during a slow annealing [parameters: system size 30^3 , cooling rate 10^5 Monte Carlo (MC) steps per unit T with lines corresponding to the legend of (d)]. The set 1 liquid crystallizes similarly to the reference liquid without competitors (lower inset). The set 2 liquid does not crystallize, but arrests into an amorphous state (upper inset shows a slice). (d) The concentration of the crystalline structure as a function of the inverse temperature for these three systems. Dotted lines indicate the leading order in $1/T$ with slope Q , the liquid’s affinity to the crystalline structure, as predicted from Eq. (2).

energy per site is thus

$$E = \sum_{\text{structures } i} c_i \epsilon_i, \quad (1)$$

where c_i is the fraction of sites in local structure i . We study this model by canonical ensemble simulations using the Monte Carlo (MC) Metropolis algorithm with single spin flips, in a periodic box with typical dimensions 30^3 .

In a previous study [13], we have studied the simplest case where a single $\epsilon_i = -1$ for a selected favored local structure, while all other structures have zero energy. In this case, the energy per site is simply minus the concentration of the FLS, and the ground state is the densest packing of the FLS. Because structures at nearby sites overlap and thus exert constraints on each other, these ground states can be highly frustrated (i.e., the selected FLS cannot fully “tile” the lattice) and the maximum FLS fraction varies between $1/4$ and 1 . As we have shown [13], this frustration does *not* prevent crystallization on moderately slow annealing of the system, leading us to conclude that some kind of *competition* between structures—in other words, multiple minima in the local energy landscape—is required to stabilize the liquid. Indeed, we have established more recently [14] that favoring simultaneously two or more of the highly frustrated structures can prevent crystallization even at very slow cooling rates, resulting in the dynamic arrest of an amorphous state at low temperature.

In this article, we use a variant of the FLS model adapted to study the role of competing structures in the crystallization of a supercooled liquid, as illustrated in Fig. 1(a). A *crystalline local structure* (denoted by XS) competes with a small number $n = 2, \dots, 10$ of *frustrated competing structures*. All these structures are given an energy $\epsilon = -1$, while other structures have zero energy. For simplicity, the crystalline structure is chosen to be the all-up structure, whose ground state is unambiguously a uniform configuration of up spins, with energy -1 per site. The mix of competitors is selected such that it does not lead to the formation of alternate metastable

crystals, but continuously arrests (in the absence of the XS) into a high-energy amorphous state with high energy $E > -0.6$ (see Appendix).

III. INTRODUCING THE CRYSTAL AFFINITY

An example demonstrates that the geometry of the frustrated competitors can substantially influence the rate of crystallization of the liquid. In Fig. 1(b) we present two apparently similar sets of $n = 6$ frustrated structures (sets 1 and 2) that we choose as competitors to the all-up crystalline structure. In Fig. 1(c) we compare the behavior of $E(T)$ of these two systems on slow cooling with that of a reference liquid in which only the crystalline structure is favored. In this latter case (black curve) the system exhibits little ordering in the liquid (less than 0.1% of XS) prior to a sharp first-order transition to the uniform ground state (lower inset). Adding set 1 of competing structures, the liquid is much more ordered and accumulates up to 12% of FLS, before freezing into the uniform ground state too. In contrast, set 2 results in similar liquid energetics, but an absence of crystallization: at low temperature, the system arrests into an amorphous state with no trace of long-range ordering [upper inset of Fig. 1(c)] in which 43% of the sites are in a favored structure. We estimate the fastest nucleation rate of each of these systems and find that the reference liquid (i.e., that with only the XS favored local structure) freezes in $\tau_{\text{nucl}} \approx 7.10^4$ MC steps; with set 1 favored, freezing is actually slightly faster with $\tau_{\text{nucl}} \approx 4.10^4$, while with set 2 we find that $\tau_{\text{nucl}} > 10^{12}$ steps: we never observe crystallization for this system in our simulations.

How can slight geometrical changes in the competing structures slow down crystallization by more than seven decades? The origin of this difference does not lie in the thermodynamic stability of the liquid: they have comparable liquid energies and identical ground states. They also have similar liquid relaxation times ($\tau_\alpha < 10$ MC steps per site). Their crucial difference is revealed by considering the liquid

structure. In Fig. 1(d) we plot the fraction c_{XS} of sites in the crystalline structure for each of these systems as a function of $1/T$. On cooling, we find that the set 1 liquid accumulates significantly *more* crystalline order than the reference liquid: the competitors actually help the liquid accumulating XS, a behavior that we label as *agonist* towards crystallization. The set 2 liquid, in contrast, *antagonizes* crystallization by suppressing local crystalline order: in spite of the XS being favored with energy -1 , their concentration actually decreases when cooling a liquid from the random infinite-temperature limit. This observation intuitively explains the dramatic difference in crystal nucleation rates in these two systems: crystalline local structures are a necessary precursor to freezing, hence their suppression can be expected to make crystallization extremely difficult.

We now propose a general statistical measure of the liquid structure that can quantitatively differentiate liquids like our set 1 and set 2 examples. A high-temperature expansion of the concentration of local crystalline structures

$$c_{XS}(T) = c_{XS,\infty} + \frac{Q}{T} + O(T^{-2}) \quad (2)$$

already captures the distinction between crystal-agonist and -antagonist systems through the value of the first-order coefficient Q , which we call the *crystal affinity* of this liquid. Denoting by Q_0 the affinity of the reference liquid with only the XS favored, agonist systems have $Q > Q_0$ and antagonists $Q < Q_0$ [dotted lines in Fig. 1(d)]. In a previous work [14], we have developed an approach, that we termed *structural covariance*, to compute exactly such high-temperature coefficients in terms of geometrical overlap of structures. Indeed, we have shown the following fluctuation-response-like relation:

$$Q = \left. \frac{\partial c_{XS}}{\partial \beta} \right|_{T=\infty} = - \sum_{\text{structures } i} C_{XS,i} \epsilon_i, \quad (3)$$

where $\beta = 1/T$, and the coefficients $C_{XS,i}$ quantify the geometrical interactions between the XS and all structures i (including the XS itself). These coefficients are equal to the covariances of structural concentrations,

$$C_{i,j} = N \text{cov}_{T=\infty}(c_i, c_j), \quad (4)$$

where N is the system size (making $C_{i,j}$ size independent), and the covariance is computed at infinite temperature, i.e., on completely random spin configurations. In this regime, correlations between structures only occur when structures overlap and share sites, exerting athermal constraints on each other, as sketched in Fig. 2(a). We emphasize that the crystal affinity Q is determined by the degree with which the various favored local structures exclude the crystal local structures from their surrounding space. An FLS that can hardly overlap with the crystal structure will diminish Q while one that overlaps well with the crystal structure in a variety of orientations will act to increase Q . The crystal affinity Q , in other words, reflects the *entropic* constraints that affect the density of local crystalline structures in the liquid (i.e., a low Q corresponds to a liquid whose FLS impose a high entropic cost on crystalline fluctuations). The covariances between structures can be either measured by

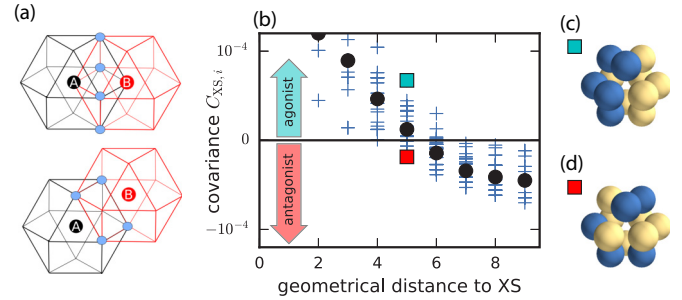


FIG. 2. (a) Nearby structures on the lattice overlap and share sites (blue dots), giving rise to athermal correlations. (b) Structural covariance between the crystalline structure (all up) and the 217 other structures (blue crosses) as a function of the number of spin flips required to convert this structure into the crystalline one. Black circles indicate average values. (c), (d) Two structures with five down spins, the former being an agonist [cyan square in (b)] while the latter is an antagonist (red square).

statistical analysis of high-temperature liquid configurations, or computed exactly by analyzing such overlaps [12,14]. Intuitively, similar structures will tend to overlap well and thus have a positive covariance, while very different structures will tend to exclude one from the other's vicinity. In the FLS model, we can define a *geometrical distance* between two structures as the minimum number of spin flips required to convert one local structure into the other. As shown in Fig. 2(b), the value of $C_{XS,i}$ decreases with geometrical distance between competing structure i and the XS, a trend that is not specific to this choice of crystalline structure (see the Appendix). What is also clear from Fig. 2(b) is that the geometrical distance does not fully determine the structural covariance. Structures in Figs. 2(c) and 2(d) both are five spin flips away from the XS, but the former is a strong agonist while the latter is an antagonist [respectively cyan and red squares in Fig. 2(b)]. A glimpse at their geometry explains this difference: the first has all its down spins on one side, attracting XS on the other. The antagonist, in contrast, has its down spins scattered over the structure, such that no XS can overlap with it in any of the two ways shown in Fig. 2(a). The crystal affinity Q defined in Eq. (3) therefore encodes, at a pair interaction level, the specific geometric interactions between the crystalline local structure and its frustrated competitors.

The crystal affinity Q is only a first-order term in Eq. (2), and so does not quantitatively capture the crystallite concentration at low temperature in Fig. 1(d). It does very well, however, in capturing both the degree of antagonism (or agonism) of the liquid and the variation in different liquids in c_{XS} at low temperature, as shown in Fig. 3(a). This simple geometrical quantity, therefore, provides a very useful insight into the complex structural fluctuations of the supercooled liquid. Perhaps most striking, the crystal affinity also correlates strongly with the nucleation time of the crystal in this liquid. Indeed, in Fig. 3(b) we show that varying Q in similar liquids leads to variations of τ_{nucl} over eight orders of magnitude. We remind the reader that Q contains only information about structural pair correlations obtained in the high-temperature limit.

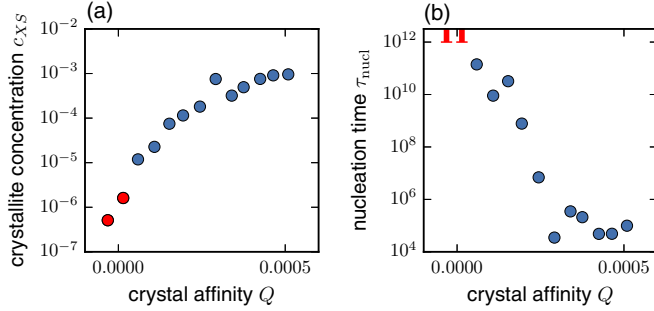


FIG. 3. (a) Influence of the crystal affinity Q [Eq. (3)] of liquids with $n = 7$ competitors on the concentration of XS, at low temperature $T = 0.6$ where nucleation is the fastest. To prevent the liquid from crystallizing, the XS was not favored in this specific plot. (b) Fastest nucleation time of the crystal as a function of Q (see the Appendix for details on the methods). The red error bar indicates no nucleation in 10^{12} MC steps. The 13 systems presented here are selected to uniformly span the range of Q values.

IV. CRYSTAL AFFINITY AND THE CLASSICAL THEORY OF CRYSTAL NUCLEATION

The mechanism by which the crystal affinity controls nucleation rates can be interpreted within the framework of classical nucleation theory (CNT) [15], in which the bulk free energy gain ΔF in crystallization is opposed by a surface free energy cost σ for the interface between the growing crystal nucleus and the supercooled liquid. In this theory, the kinetically limiting step to crystallization is assumed to be the thermally activated formation of a critical nucleus, predicting an average nucleation time

$$\tau_{\text{nucl}} = \tau_{\alpha} N \exp\left(\frac{\sigma^3}{k_B T \Delta F^2}\right), \quad (5)$$

where N is the number of potential nucleation sites and τ_{α} is the microscopic relaxation time of the supercooled liquid. There are therefore three possible ways to make crystallization slower: by slowing down the kinetics of the liquid (i.e., increasing τ_{α}), by stabilizing thermodynamically the liquid (i.e., lowering ΔF), or by increasing the liquid-crystal surface tension σ .

We have seen in Fig. 3(b) that the crystal affinity Q strongly influences the nucleation rate. In order to understand which of these aspects are affected by this affinity, we study nucleation in a large number of supercooled liquids with $n = 2$ –10 competing structures, and selected to sample uniformly the available range of Q values. As shown in Fig. 4(a), the key factor influencing nucleation times in this data set is the crystal affinity, rather than the number of competing structures. In particular, it is worth noting that for negative values of Q (a situation indicating that crystalline structures, in spite of being favored, are linearly suppressed in $1/T$ as the liquid is cooled down), crystallization is robustly suppressed and never observed in our simulations. For this whole data set, we analyze in Figs. 4(b)–4(d) the correlations between Q and each of the three aspects of the CNT nucleation rate. Strikingly, we find that Q exhibits no significant correlation with either the relaxation time τ_{α} [Fig. 4(b)] or the free energy difference ΔF [Fig. 4(c)]. It does, however, correlate very strongly with the

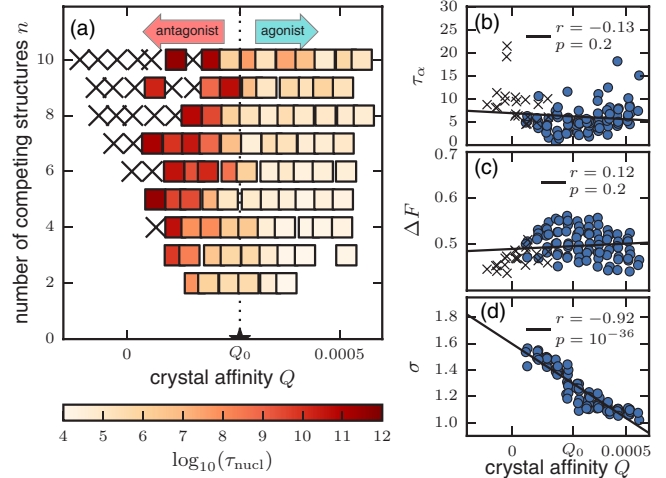


FIG. 4. (a) Nucleation rates of liquids with varying crystal affinity Q and number n of frustrated competitors, showing that it is the value of Q , rather than the number of competitors, that determines the crystallization rate. Black crosses indicate $\tau_{\text{nucl}} > 10^{12}$ MC steps. (b)–(d) Correlation between Q and the three parameters of classical nucleation theory: liquid relaxation time τ_{α} (computed as the autocorrelation time of the energy, in MC steps per site), liquid-crystal free energy difference ΔF (computed by thermodynamic integration), and liquid-crystal surface tension σ [inferred using Eq. (5) and the measured nucleation times]. The legend indicates the Pearson r coefficient and p value. The only statistically significant correlation is between Q and σ .

surface tension σ [Fig. 4(d)]: with an r coefficient of -0.92 , the surface tension is almost fully determined by Q . This effect is remarkable as it implies that, within our model, the complex problem of estimating the low-temperature surface tension σ —a quantity that is somewhat ill defined in CNT, as it is not a property at thermodynamic equilibrium, and the concept of surface is ambiguous for microscopic clusters—can be bypassed by measuring the crystal affinity Q , a simple, high-temperature structural quantity.

V. CONCLUSION

In this article, we have introduced the crystal affinity $Q = \partial c_{XS} / \partial \beta |_{T=\infty}$ as a measure of the propensity of the liquid to accumulate crystalline order on cooling, using the local crystal structure concentration c_{XS} as an inherent probe of crystallinity. This number encapsulates, in an intelligible way, the geometrical interactions of the crystal with noncrystalline stable local structures that compete with crystalline order in the liquid. Indeed, we have shown with Eq. (3) that, in a fluctuation-response-like relation, Q can be computed by analyzing the covariances in the number of crystalline and noncrystalline local structures at high temperature. Furthermore, we have demonstrated that Q provides an excellent predictor of the qualitative trends in rate of crystal nucleation: low affinity implies slow nucleation. More precisely, we have established a clear correlation between Q and the effective crystal-liquid interfacial energy (as obtained from the nucleation time data through the assumption of classical nucleation). This result raises the interesting prospect of a treatment of crystal

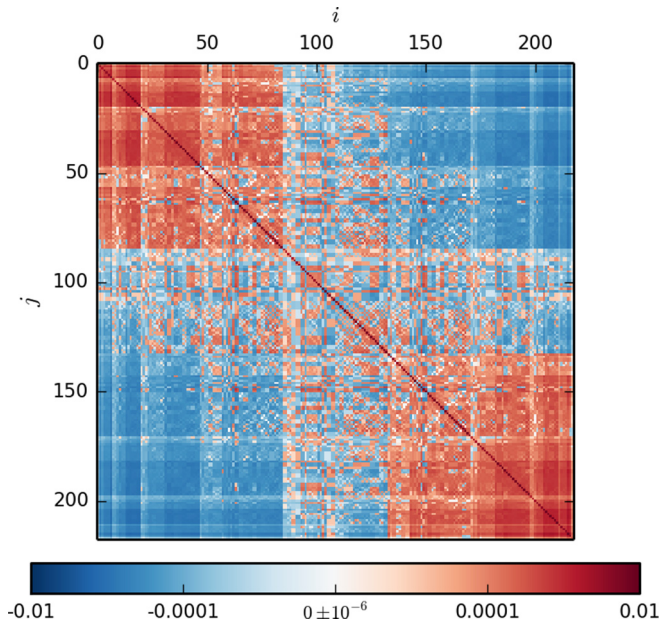


FIG. 5. The covariance matrix of the FLS model at infinite temperature, showing all coefficients $C_{i,j}$ defined in Eq. (4).

nucleation in terms of the statistics of structural fluctuations, rather than relying on the awkward imposition of a macroscopic interface. Since the only requirement for Eqs. (2)–(4) to hold is that the Hamiltonian of the system can be formulated in terms of a short-range local energy landscape, as in Eq. (1), the analysis presented here should provide a quite general framework for the systematic study of structural fluctuations in off-lattice supercooled liquids, and the influence of these fluctuations on the rate of crystal nucleation. In particular, structural covariances could be used as a guide to engineer local energy landscapes that kinetically facilitate or hinder the formation of a target crystal structure.

ACKNOWLEDGMENTS

P.R. is supported by the Princeton Center for Theoretical Science and the Prix des Jeunes Chercheurs de la Fondation des Treilles. P.H. is supported by the Australian Research Council.

APPENDIX: METHODS

Here we provide the details of the rationale and procedures associated with the specific choices of model parameters used in the paper and the properties used to characterize structural fluctuations and nucleation rates. In a previous publication [13], we have presented a detailed description of the FLS model, including a comprehensive survey of the phase behavior of the model in the cases where only a single structure is favored. Readers interested in the model are referred to Ref. [13].

a. Calculating the crystal affinity. The high-temperature covariances between concentrations of local structures, as introduced in Eq. (4), are displayed in Fig. 5. These coefficients are computed exactly using an enumerative algorithm testing for all possible overlaps between pairs of structures, as described in Refs. [14,16].

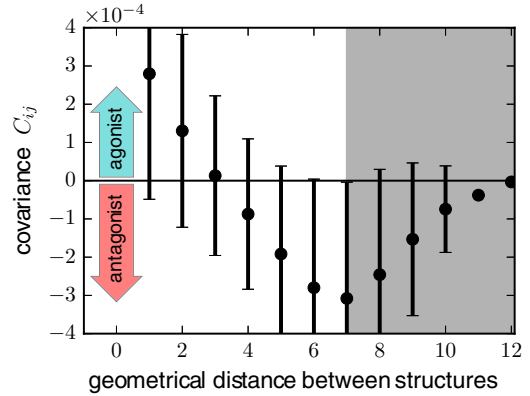


FIG. 6. The average covariance between any two structures as a function of their geometrical distance, complementing the plot in Fig. 2(b) where only the all-up structure was shown. Error bars show standard deviation. The covariances are clearly monotonically decreasing over the first seven spin flips, though with large standard deviation reflecting the importance of the geometrical distribution of the spins. The increase for distance above seven spin flips can be explained by symmetry effects (structures very far apart tend to have higher symmetry, which results in lower absolute value of the covariances as the mean concentrations are lower) and lack of data.

We show in Fig. 6 that the coefficients $C_{i,j}$ depend on geometrical distance between structures, regardless of the nature of i and j (not only for the all-up XS selected in the article).

b. Generating the liquids. We discuss here the way we generate and select the 107 liquids that are used for the statistical study in Fig. 4. These are selected randomly from a large set of possible combinations of the 74 structures depicted in Fig. 7. These structures are those of the 218 local structures in the FLS model that have the following properties: (i) a ground state energy higher than or equal to $-1/3$, ensuring that the structure is frustrated and does not permit formation of crystal polymorphs that would compete with the all-up ground state, and (ii) a number of “up” spins between 4 and 8, so that the interactions between structures rely on geometrical properties rather than on mere ferromagnetic attraction or repulsion. There are 19 distinct types of local structures (columns in Fig. 7) fulfilling these conditions, coming in up to four variants when including the mirror-and/or spin-inverted variants. For each value of the number of competing local structures $n = 2, \dots, 10$, we generate 10^4 different Hamiltonians by picking randomly one structure in n randomly selected columns of Fig. 7. (We do not use two structures of the same column as we observed empirically that this tends to increase crystallization of composite metastable crystals.) We then pick samples that are regularly spaced in values of Q , so as to investigate the correlation between Q and thermodynamic observables. These samples are selected by binning the 10^4 systems by values of Q , with interval 1.5×10^{-5} . We then pick one system in one bin out of three, thus obtaining a first batch of 107 Hamiltonians (not all values of (Q,n) are possible).

We are interested in nucleation of the target crystal structure (the all-up system) within a liquid where the competitors are present too. We thus run a preselection simulated annealing,

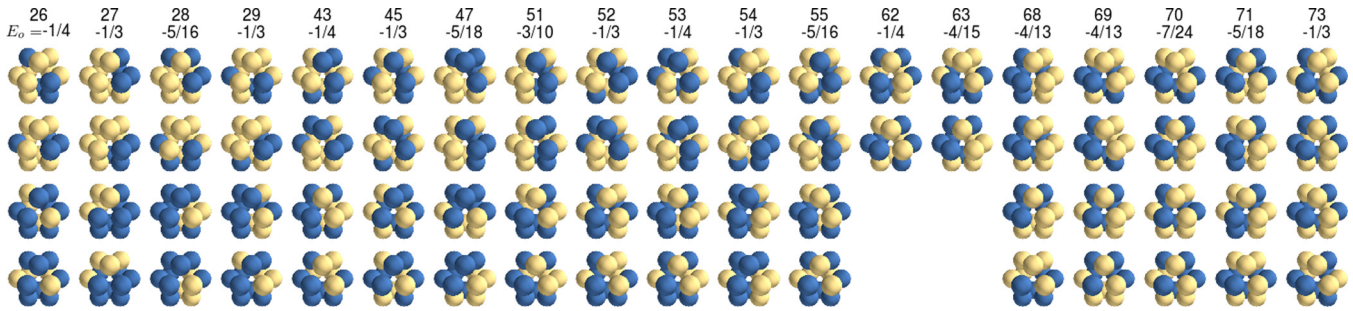


FIG. 7. The 19 choices of local structures used to generate the liquids studied in Figs. 3 and 4, with their label as in Ref. [13] and the corresponding ground state energy per site (minus the maximum fraction of sites that can be in the corresponding structure). Each column represents the spin- and mirror-inverted variants of the same structures, which on their own have identical properties, but have different packing properties when combined with other structures. Structures 62 and 63 have an additional symmetry (respectively spin inversion, and spin inversion combined with mirror symmetry) and thus have only two variants. Structures 26–29 have four spins down; structures 43–55 have five; and structures 62–73 have six spins up and six down. Extensive details about these structures can be found in the supplementary information of Ref. [13].

with only the frustrated competing structures favored (no XS), to eliminate those of these systems that tend to crystallize into a polymorph crystal made of a combination of the frustrated competing structures and thus would not remain liquid at temperatures near the point at which we study nucleation, $T = 0.6$. We thus eliminate and repick the system to obtain another Hamiltonian with similar Q value if, on slow annealing, (i) the system exhibits a sharp first-order phase transition apparent as a discontinuity in energy per site $E(T)$; (ii) the system exhibits a peak of heat capacity at $T > 0.45$ (sign of either a weakly first-order phase transition, or a second-order transition that would result in (near-)critical slowdown of the kinetics, and hence affect the nucleation rate in an undesired way; or (iii) the system exhibits obvious long-range crystalline ordering in the final, low-temperature state. Once these preselection tests and repicking are performed, we have obtained a large set of 107 Hamiltonians composed of a mixture of the structures depicted in Fig. 7, regularly spaced in Q and n values, that do not, when only these structures are favored, crystallize on cooling. This phenomenology is further described in Ref. [14] in the case of mixtures of two frustrated FLS. Note that the 13 systems presented in Fig. 3 are simply the $n = 7$ line in Fig. 4.

c. Measuring nucleation times. We can next measure nucleation times for each of these Hamiltonians. Our protocol is the following: We prepare the liquid in a system of 20^3 sites with periodic boundary conditions, by annealing a similar system, but without favoring the XS so as to prevent premature nucleation. Having such an equilibrated liquid, we check that it has not crystallized into a frustrated polymorph (i.e., that the system’s energy is consistent with the corresponding liquid), then add the XS to the set of favored structures. We then perform MC moves at a fixed temperature $T = 0.6$ (chosen to be the temperature of fastest nucleation, in a quite robust way) until crystallization is detected, i.e., when the energy falls below a threshold energy of -0.9 , from which the system always falls into the ground state. This protocol is, however, spoiled by the presence of ballistic relaxation, both before nucleation (relaxation of the liquid after adding the XS) and after nucleation (crystal growth). For short nucleation times, this makes the measured time before hitting the threshold strongly reproducible. We thus obtain an upper bound to the

nucleation time by repeating the simulation several times (up to 20 times or 10^{12} MC steps) and measuring the standard deviation of the crystallization time, which gives us an estimate of τ_{nucl} , assuming that nucleation times are exponentially distributed (i.e., no aging or memory in the liquid prior to nucleation).

d. Liquid relaxation times. The relaxation times τ_α of the liquid [as presented in Fig. 4(b)] are the autocorrelation times of the energy of the liquid, expressed in Monte Carlo steps per site. They are obtained using the batch autocorrelation method.

e. Free energies. Liquid-crystal free energy differences presented in Fig. 4(c) are computed by approximating the crystal’s free energy by its energy value $E \approx -1$, neglecting its entropy. An approximation of the liquid free energy is obtained by thermodynamic integration from infinite temperature of the system without the XS favored, so that it does not crystallize in the annealing run performed to integrate the free energy. Neglecting the XS leads to a minor error in the free energy of the liquid (less than 1% in systems for which crystallization is slow enough to allow measurement of the free energy with the XS favored).

f. Surface tensions. We do not measure directly the surface tensions presented in Fig. 4(d); rather, we infer it through the

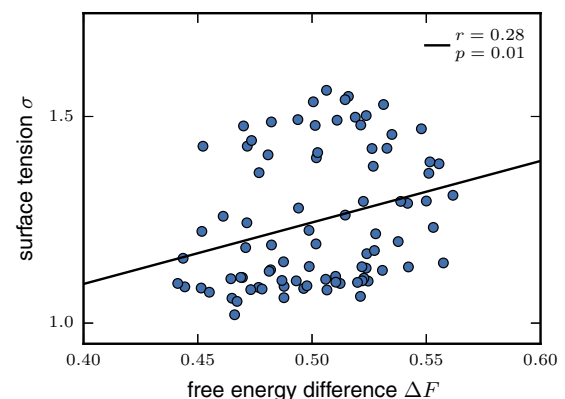


FIG. 8. Correlations between the liquid-crystal surface tension and bulk free energy difference are negligible within our data set.

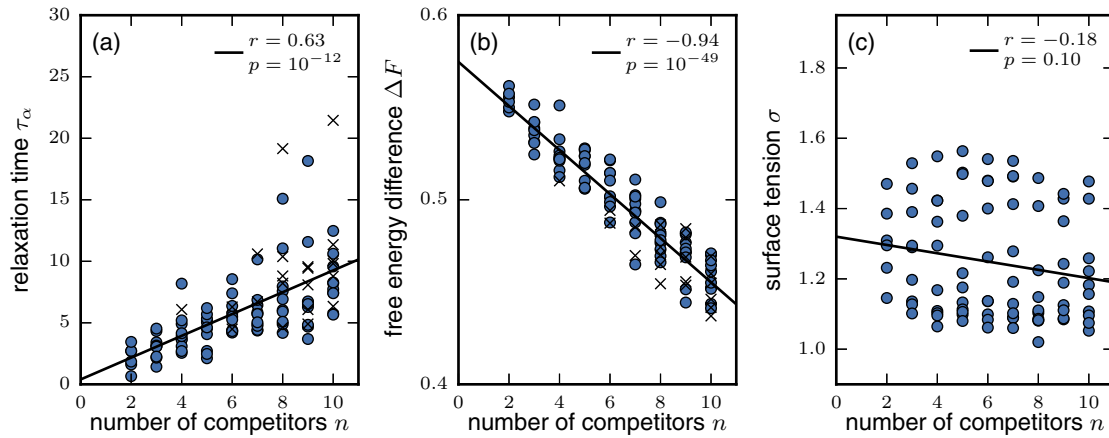


FIG. 9. Correlations between number of competing structures, n , and parameters of the classical nucleation theory that influence the nucleation time. The data set is the same as in Fig. 4.

classical nucleation theory assumption, using

$$\sigma \approx [k_B T \Delta F^2 \log(\tau_{\text{nucl}}/\tau_\alpha)]^{1/3}, \quad (\text{A1})$$

where $k_B = 1$ in our unit system, $T = 0.6$ for all nucleation runs presented in this article, and τ_{nucl} , τ_α , and ΔF are obtained as discussed above. Note that we do not include the volume factor $N = 20^3$ in Eq. (A1); doing so would result in undefined values for σ for many of the high-affinity liquids, as nucleation is often faster than $N\tau_\alpha$ in these cases. In any case, σ in this article should not be interpreted too strictly as a surface tension; as discussed at the end of the main text, this notion is somewhat ill defined, on top of being particularly difficult to measure directly. Rather, it quantifies the aspect of the nucleation rate that is not a consequence of the bulk free energy gain ΔF in crystallizing, as illustrated in Fig. 8 by showing the near absence of correlation between σ and ΔF .

g. Influence of the number of competitors. In Fig. 4, we present a large data set of liquids with varying number

of competing structures n and crystal affinity Q . Figures 4(b)–4(d) analyze the influence of Q on the different parameters τ_α , ΔF , and σ that affect the nucleation time, showing that Q strongly correlates with σ while being essentially independent of the other parameters. As a complement, we present in Fig. 9 the same correlations, but with the other parameter of our data set, the number of frustrated competing structures, n . It presents a strong correlation with ΔF ($r = 0.94$), while showing no significant correlation to σ . These results can be intuitively understood by noting that adding more competitors to the liquid increases the number of ways for the liquid to lower its energy: it will thus increase its entropy, at a given energy, and thus lower the free energy of the liquid, while leaving the crystal unaffected. On the other hand, these additional competitors are equally likely to act as agonist or antagonist with the crystalline structure; hence they do not significantly affect the crystal affinity Q and, therefore, do not affect the surface tension either.

-
- [1] F. C. Frank, *Proc. R. Soc. London A* **215**, 43 (1952).
 [2] C. P. Royall and S. R. Williams, *Phys. Rep.* **560**, 1 (2015).
 [3] Y. Q. Cheng and E. Ma, *Prog. Mater. Sci.* **56**, 379 (2011).
 [4] G. Tarjus, S. A. Kivelson, Z. Nussinov, and P. Viot, *J. Phys.: Condens. Matter* **17**, R1143 (2005).
 [5] H. W. Sheng, W. K. Luo, F. M. Alamgir, J. M. Bai, and E. Ma, *Nature (London)* **439**, 419 (2006); J. Ding, E. Ma, M. Asta, and R. O. Ritchie, *Sci. Rep.* **5**, 17429 (2015).
 [6] A. C. Y. Liu, R. F. Tabor, L. Bourgeois, M. D. de Jonge, S. T. Mudie, and T. C. Petersen, *Phys. Rev. Lett.* **116**, 205501 (2016); A. Hirata, J. J. Kang, T. Fujita, B. Klumov, K. Matsue, M. Kotani, A. R. Yavari, and M. W. Chen, *Science* **341**, 376 (2013).
 [7] H. Shintani and H. Tanaka, *Nat. Phys.* **2**, 200 (2006); M. Leocmach, J. Russo, and H. Tanaka, *J. Chem. Phys.* **138**, 12A536 (2013).
 [8] J. Taffs and C. P. Royall, *Nat. Commun.* **7**, 13225 (2016).
 [9] V. Molinero, S. Sastry, and C. A. Angell, *Phys. Rev. Lett.* **97**, 075701 (2006).
 [10] G. W. Lee, A. K. Gangopadhyay, T. K. Croat, T. J. Rathz, R. W. Hyers, J. R. Rogers, and K. F. Kelton, *Phys. Rev. B* **72**, 174107 (2005).
 [11] P. Ronceray and P. Harrowell, *Europhys. Lett.* **96**, 36005 (2011).
 [12] P. Ronceray and P. Harrowell, *J. Chem. Phys.* **136**, 134504 (2012).
 [13] P. Ronceray and P. Harrowell, *Soft Matter* **11**, 3322 (2015).
 [14] P. Ronceray and P. Harrowell, *J. Stat. Mech.* (2016) 084002.
 [15] K. F. Kelton and A. L. Greer, *Nucleation in Condensed Matter* (Elsevier, Amsterdam, 2010).
 [16] P. Ronceray and P. Harrowell, *Mol. Simul.* **42**, 1149 (2016).